HHS Public Access

Author manuscript

Hepatology. Author manuscript; available in PMC 2023 April 25.

Published in final edited form as:

Hepatology. 2022 November ; 76(5): 1248–1258. doi:10.1002/hep.32536.

Identification of the chloride channel, leucine-rich repeat-containing protein 8, subfamily a (LRRC8A), in mouse cholangiocytes

Nikolay Shcheynikov[1], **Kristy Boggs**[1], **Anthony Green**[2], **Andrew P. Feranchak**[1,3]

[1]Department of Pediatrics, University of Pittsburgh Medical Center Children's Hospital of Pittsburgh, Pittsburgh, Pennsylvania, USA

[2]Tissue and Research Pathology Core, UPMC Hillman Cancer Center, University of Pittsburgh, Pittsburgh, Pennsylvania, USA

[3]Pittsburgh Liver Research Center, University of Pittsburgh, Pittsburgh, Pennsylvania, USA

Abstract

Background and Aims: Chloride (Cl^-) channels in the apical membrane of biliary epithelial cells (BECs), also known as cholangiocytes, provide the driving force for biliary secretion. Although two Cl^- channels have been identified on a molecular basis, the Cystic Fibrosis Transmembrane Conductance Regulator and Transmembrane Member 16A, a third Cl^- channel with unique biophysical properties has been described. Leucine-Rich Repeat-Containing Protein 8, subfamily A (LRRC8A) is a newly identified protein capable of transporting Cl^- in other epithelium in response to cell swelling. The aim of the present study was to determine if LRRC8A represents the volume-regulated anion channel in mouse BECs.

Approach and Results: Studies were performed in mouse small (MSC) and large (MLC) cholangiocytes. Membrane Cl^- currents were measured by whole-cell patch-clamp techniques and cell volume measurements were performed by calcein-AM fluorescence. Exposure of either MSC or MLC to hypotonicity (190 mOsm) rapidly increased cell volume and activated Cl^- currents. Currents exhibited outward rectification, time-dependent inactivation at positive membrane potentials, and reversal potential at 0 mV (E_{Cl}). Removal of extracellular Cl^- or specific pharmacological inhibition of LRRC8A abolished currents. LRRC8A was detected in both MSC and MLC by reverse transcription polymerase chain reaction and confirmed by western blot. Transfection with LRRC8A small interfering RNA decreased protein levels by >70% and abolished volume-stimulated Cl^- currents.

Correspondence: Andrew Feranchak, Rangos Research Center, University of Pittsburgh Medical Center Children's Hospital of Pittsburgh, 7th Floor, 4401 Penn Ave., Pittsburgh, PA 15224, USA. andrew.feranchak@chp.edu.

AUTHOR CONTRIBUTIONS

Nikolay Shcheynikov, Kristy Boggs, and Andrew P. Feranchak were responsible for conceptualization; Nikolay Shcheynikov, Kristy Boggs, and Andrew P. Feranchak were responsible for methodology; Nikolay Shcheynikov and Kristy Boggs were responsible for investigation; Anthony Green was responsible for the immunohistochemistry; and Nikolay Shcheynikov, Kristy Boggs, and Andrew P. Feranchak were responsible for writing (review and editing).

SUPPORTING INFORMATION

Additional supporting information may be found in the online version of the article at the publisher's website.

CONFLICT OF INTEREST

Nothing to report.

Conclusion: These results demonstrate that LRRC8A is functionally present in mouse BECs, contributes to volume-activated Cl^- secretion, and, therefore, may be a target to modulate bile formation in the treatment of cholestatic liver disorders.

INTRODUCTION

Bile formation is initiated by hepatocyte transport of bile acids into the canalicular space between cells. Subsequently, canalicular bile enters an extensive intrahepatic network of ducts lined by biliary epithelial cells (cholangiocytes), which modify the volume and composition of bile through regulated ion and water secretion. Despite the small number of cholangiocytes, the network of intrahepatic ducts is extensive, and ductular secretion is estimated to contribute to over 40% of bile volume in humans.[1–3] Opening of Cl^- channels in the apical membrane of cholangiocytes provides the driving force for biliary secretion,[4–6] and our laboratory has previously identified three Cl^- channel types based on biophysical properties, though in only two were the molecular identities defined: the Cystic Fibrosis Transmembrane Conductance Regulator (CFTR), a cAMP-activated Cl^- channel, and Transmembrane Member 16A protein (TMEM16A), a Ca^{2+}-activated Cl^- channel.[7,8]

Although CFTR is activated by the hormone secretin binding basolateral receptors, TMEM16A is activated by mechanical stimuli acting on the apical membrane in a process involving ATP release and binding of apical purinergic receptors. Interestingly, stimuli, which exert mechanical effects on the apical membrane also activate a third type of Cl^- channel with unique biophysical properties, including activation by cell swelling and time-dependent inactivation at positive membrane potentials.[9–11] This channel has previously been named the volume-regulated Cl^- channel or the volume-regulated anion channel (VRAC).

All cells must be able to respond to changes in the osmolarity of their environment in order to maintain membrane and cellular integrity. The process by which cells respond to stimuli, which increase cell size and return the cell to near basal size, is known as regulatory volume decrease (RVD). RVD is especially critical for cells of the liver, which are exposed to changes in osmolarity between fed and fasted states.[12,13] The process of RVD is characterized by activation of membrane Cl^- and K^+ channels, water efflux, and a return to near basal size.[14] Although we have previously shown that a human biliary cell model undergoes RVD and activates membrane Cl^- channels,[15] the molecular identity of this Cl^- channel is unknown.

One of the critical components of VRAC responsible for RVD in other cells has been identified as the Leucine-Rich Repeat-Containing Protein 8, subfamily A (LRRC8A) and therefore a component of the regulated response to cell swelling.[9,16] However, it is unknown if LRRC8A is present or functional in cholangiocytes. The aim of the present study therefore was to determine if LRRC8A represents a critical component of the VRAC in mouse cholangiocytes.

EXPERIMENTAL PROCEDURES

Cell models

As primary isolated mouse cholangiocytes lose biophysical properties in culture quite rapidly, patch-clamp studies were performed in mouse large cholangiocytes (MLC) and mouse small cholangiocytes (MSC), which were obtained from Drs. Alpini and Glaser. In brief, cholangiocytes were isolated from normal mice (BALB/c) and immortalized by transfection with the SV40 large-T antigen gene as described.[17,18] These cells demonstrate similar properties to those of freshly isolated small and large mouse cholangiocytes. Importantly, MSC do not express CFTR, whereas MLC do, and both cell types functionally express TMEM16A.[8,17] To isolate primary cholangiocytes, the bile duct of a C57BL/6 mouse was perfused with collagenase D, the liver was removed, and the bile duct was carefully dissected out along the intrahepatic ducts with the physical removal of nonduct tissue. The bile duct was minced and trypsinized overnight to release cells from the bile duct. Cholangiocytes were enriched for using CD326 (EpCAM) Magnetic MicroBeads, an MS Column, and MiniMACS Separator (Miltenyi Biotec) per the manufacturers' protocol. Animal work described in this manuscript has been approved and conducted under the oversight of the University of Pittsburgh Institutional Animal Care and Use Committees.

Detection of Lrrc8 paralogs by reverse transcription polymerase chain reaction

RNA was extracted from the cells using Trizol (Invitrogen) followed by a DNase I treatment using the RNA Clean and Concentrator Kit (Zymo Research, catalog no. R1013). The DNase I-treated RNA (1 μg) was converted to complementary DNA (cDNA) using iScript Reverse Transcription Supermix (Bio-Rad, catalog no. 1708840) per the manufacturer's instructions. The cDNA was diluted 1:4 with water. PCR products representing the Lrrc8 paralogs (Lrrc8a–e) were detected with a 20 μl PCR reaction mixture containing sequence-specific primers (Table S1), GoTaq Master Mix (Promega, catalog no. M7132), and a 1/20 volume of cDNA. The mixture was subjected to 35 cycles of amplification (denaturation at 95°C for 30 s, annealing at 56°C for 30 s, and extension at 72°C for 20 s). The amplified DNA was resolved on a 2% agarose gel alongside a 50 bp ladder.

Localization of LRRC8A protein by immunohistochemistry staining

Localization of LRRC8A protein was performed on paraffin-embedded mouse liver tissue. The slides were heated to 60°C for 30 min followed by deparaffinization and rehydration using a standard histology protocol: three changes of xylene for 5 min each followed by three changes of 100% alcohol, two changes of 95% alcohol, and one change of 70% alcohol, each for 1 min, and then rinsed in distilled water. Antigen retrieval was performed using a citrate buffer (#S1699, Agilent Dako) in a Decloaking Chamber (Biocare Medical). The slides were stained using an Autostainer Plus (Agilent Dako) platform with TBST rinse buffer (#S3306, Agilent Dako). The primary antibody, LRRC8A (Table S2), was applied at 1:200 dilution, at room temperature for 60 min. The secondary antibody, Envision Rabbit HRP polymer (Table S2), was applied for 45 min at room temperature. The substrate, 3,3′-diaminobenzidine + (#K3 468, Agilent Dako), was applied for 10 min. The slides were counterstained with hematoxylin (#K8018, Agilent Dako). Negative controls were performed as described above minus the primary antibody incubation.

Small interfering RNA knockdown of Lrrc8a gene expression

Lrrc8a gene expression (and subsequently protein expression) was suppressed by transient transfection (Invitrogen, Lipofectamine 2000 Transfection Reagent, catalog no. 11668027) of cells with an LRRC8A small interfering RNA (siRNA; Invitrogen, Assay ID #MSS280623). A noncoding Stealth RNAi (Invitrogen, catalog no. 12935–300, medium GC duplex) was used in control transfections. Block-it Fluorescent Oligo (Invitrogen, catalog no. 2013) generates a detectable FITC signal and was used to monitor transfection efficiency and to aid in the selection of siRNA transfected cells for whole-cell patch-clamp current recording. Whole-cell patch-clamp experiments were performed 48 h after transfection on FITC-positive cells. The degree of LRRC8A silencing was evaluated by western blot analysis on FITC-positive cells that were collected by fluorescence-activated cell sorting.

Fluorescence-activated cell sorting

For western blot analysis, we sorted for FITC-positive cells in both the control and LRRC8A siRNA transfected cells. To assess cell viability, single-cell suspensions were stained with Zombie Aqua Viability Dye (Biolegend, catalog no. 423101) washed in Cell Staining Buffer (Biolegend, catalog no. 420201) and resuspended in flow cytometry buffer (PBS without calcium and magnesium, 1% BSA, 2 mM EDTA, 25 mM HEPES). Data acquisition and the subsequent collection of FITC-positive cells was performed on a Becton, Dickinson and Company (BD Biosciences) FACSAria II (BD Biosciences) and analyzed with BD FACSDiva 8.0.1 software (BD Biosciences).

Detection of LRRC8A protein by western blot

Protein was extracted from FITC-positive cells, primary cholangiocytes, and hepatocytes with RIPA buffer containing protease inhibitors (Roche) and subsequently quantified with the BCA Assay Kit (Thermo Fisher Scientific). Equal concentrations of protein were separated on 4%–15% gels (Bio-Rad), then transferred to 0.22 μm supported nitrocellulose paper (Bio-Rad). Membranes were blocked in 5% nonfat dry milk, then incubated overnight at 4°C in primary antibody (Table S2) followed by a 1 h incubation at room temperature in HRP-conjugated secondary antibody (Table S2). Signals were visualized through Amersham ECL Western Blotting Detection Reagents (GE Healthcare, catalog no. RPN2209) and band intensity quantified using ImageJ software (National Institutes of Health).

Measurement of Cl^- currents

Coverslips with MLC or MSC cells were transferred to the recording chamber and perfused with a standard external solution with the following composition (in millimolars): 145 sodium chloride (NaCl), 1 calcium chloride ($CaCl_2$), 1 magnesium chloride ($MgCl_2$), 10 HEPES, and 10 D-glucose, pH 7.4 (sodium hydroxide [NaOH]). Cl^--free solution was prepared by replacing Cl^- with gluconate. Osmolarity was adjusted with mannitol to 310 ± 5 mOsm using the Advanced Micro Osmometer (Model 3300, Advanced Instruments Inc.). For measuring swelling-activated currents and volume changes, an isotonic solution containing (in millimolars) 85 NaCl, 1 $CaCl_2$, 1 $MgCl_2$, 10 HEPES, 120 D-mannitol, and 10 D-glucose, pH 7.4, with NaOH (310 ± 5 mOsm) was used and cell swelling was induced by omitting mannitol from the solution to reach osmolarity indicated (190

mOsm for most volume-activated studies). Patch-clamp experiments were performed in the standard whole-cell configuration at room temperature (22°C–25°C) using an Axopatch 200B amplifier (Axon Instruments). Patch pipettes had resistances between 4 and 6 mΩ after filling with the standard intracellular solution that contained the following (in millimolars): 90 cesium (Cs)-chloride, 50 Cs-aspartate, 1 Mg-ATP, 10 HEPES, and 2 EGTA, pH 7.3 (cesium hydroxide). Digidata −1440A and pClamp 10 software (Molecular Devices) were used for data acquisition and analysis. The current was recorded by 400-ms rapid alteration of membrane potential from −100 to +100 mV every 2 s from a holding potential of 0 mV. The current recorded at +100 mV was used to calculate the maximum current density (pA/pF). To observe the voltage and time dependency of the current profile, step pulses were applied from a holding potential of 0 mV to test potentials of −100 to +100 mV in +20 mV increments. The current was filtered at 1 kHz and sampled at 10 kHz. Capacitive currents and series resistance were determined and minimized. Results are compared with control studies measured on the same day to minimize any effects of day-to-day variability and reported as current density (pA/pF) to normalize for differences in cell size. Data are presented as mean ± SE. Origin 2018 (OriginLab) was used for data analysis and display.

Capacitance measurements

To simultaneously measure the capacity of the cell membrane and current, the amplifier readings were used as well as the current value at +100 mV (step-by-step protocol), recorded every 30 s under iso- and hypotonic conditions. To increase the measurement accuracy, the minimum capacitance values indicated by the amplifier were used.

Cell volume measurements

Forty-thousand cells were plated the day before on a 24-well black Visiplate with a clear bottom (Perkin Elmer, catalog no. 1450–605) coated with poly-L-lysine. Cells were incubated for 1 h at 37°C in Opti-MEM containing 10 μm calcein-AM (Invitrogen, catalog no. 3100MP) or without calcein-AM to subtract for background and autofluorescence. The cells were then washed three times with 310 mOsm isotonic solution containing (in millimolars) 42 NaCl, 4 potassium chloride (KCl), 1 $CaCl_2$, 1 $MgCl_2$, 1 KH_2PO_4, 10 HEPES pH 7.4, 10 D-Glucose, and 180 D-Mannitol, followed by a 20 min room temperature incubation in the isotonic solution. Following the 20 min incubation in isotonic solution, the plate of cells was read on a Synergy H1 fluorescent plate reader (BioTek Instruments, Inc.) with an excitation of 488 nm and an emission of 520 nm every 30 s for 3 min to establish a baseline isotonic fluorescence reading. Next, the isotonic solution was replaced with either fresh 310 mOsm isotonic solution, 100 mOsm hypotonic solution containing (in millimolars) 42 NaCl, 4 KCl, 1 $CaCl_2$, 1 $MgCl_2$, 1 KH_2PO_4, 10 HEPES pH 7.4, and 5 D-Glucose, or a 100 mOsm hypotonic solution containing 4-[(2-butyl-6,7-dichloro-2-cyclopentyl −2,3-dihydro-1-oxo-1H-inden-5-yl) oxy] butanoic acid (DCPIB; 1, 10, or 20 μm). Then, the fluorescence of calcein-AM within the cells was recorded over a 47 min period of time. The change in cell volume was reported relative to the baseline isotonic reading.

Reagents

The specific LRRC8A inhibitor, DCPIB was purchased from Tocris Bioscience, and all other chemicals were obtained from Sigma-Aldrich.

Statistics

Results are presented as the mean ± SE, with *n* representing the number of culture plates or repetitions for each assay as indicated. Student's paired or unpaired *t* test or analysis of variance for multiple comparisons was used to assess statistical significance as indicated, and *p* values < 0.05 were considered to be statistically significant. Additional detailed methods are supplied in the Supplemental Material.

RESULTS

Mouse biliary epithelial cells express a functional volume-activated Cl^- channel

Exposure of either MSC or MLC to hypotonicity (190 mOsm) activated membrane Cl^- currents (MLC data are shown in Figure 1, whereas data for MSC are shown in Figure S1). Under isotonic conditions, current density was small (4.5 ± 0.5 pA/pF), but on hypotonic exposure (190 mOsm), currents activated rapidly (within 1.2 ± 0.53 min) and reached a maximum current density of 49.5 ± 3.8 pA/pF, (n = 18) by 2.5 ± 0.75 min (Figure 1A). As shown in Figure 1B,C, currents exhibited outward rectification, time-dependent inactivation at positive membrane potentials, and a reversal potential at 0 mV (E_{Cl^-}), properties consistent with LRRC8A in other cell types.[9,16] The effects of hypotonic exposure were fully reversible following return to isotonic conditions. No differences were observed in the magnitude or biophysical features between MSC or MLC cells. To confirm that the currents were mediated by Cl^- efflux, similar experiments were performed in the presence or absence of Cl^- in the buffers. As shown in Figure 2A,B, when Cl^- was removed from the buffer solutions, hypotonic-stimulated currents were abolished, confirming Cl^- as the predominant charge carrier.

Pharmacologic inhibition of LRRC8A abolishes volume-activated Cl^- currents

To determine if LRRC8A contributes to the observed volume-regulated Cl^- currents, similar experiments to those described above were performed in the presence or absence of the LRRC8/VRAC antagonist, DCPIB.[19] As shown in Figure 3, exposure of MLC to hypotonic buffer (190 mOsm) again rapidly activated Cl^- currents with a maximum current density of 55.5 ± 3.8 pA/pF in control cells. In contrast, when MLC were treated with DCPIB (10 μm), hypotonic-stimulated Cl^- currents were abolished (Figure 3A). K_m (2.1 + 0.35 μm) determined by fitting DCPIB concentration-response relationships (Figure 3B) corresponds to the K_m value (2.3 + 0.0 μM) obtained for the native VRAC in wild-type HCT116 cells.[20] In contrast, the Ca^{2+}-activated Cl^- channel inhibitor, niflumic acid (NFA), had negligible effects on volume-activated Cl^- currents (Figure 3C,D). MSC demonstrated a similar sensitivity to DCPIB (Figure S1). Together, these results demonstrate that both small and large mouse cholangiocytes exhibit volume-activated Cl^- currents that are sensitive to the LRRC8/VRAC antagonist, DCPIB.

Expression of LRRC8A mRNA and protein in biliary epithelium

We analyzed MSC and MLC cells for gene expression of the Lrrc8 paralogs (Lrrc8a–e) by reverse transcription polymerase chain reaction (RT-PCR) (Figure 4A). Lrrc8a was present in both MLC and MSC as were Lrrc8b–d. However, Lrrc8e was not detected by RT-PCR at a significant level in either cell line (Figure 4A). The LRRC8A protein is a critical component for mediating volume-regulated anion currents.[21] LRRC8A requires heteromerization with at least one of the other LRRC8 proteins (LRRC8B–E) to form a functional channel.[22] Immunostaining of whole mouse liver revealed LRRC8A in both hepatocytes and cholangiocytes (Figure 4B). Additionally, western blot analysis detected the LRRC8A protein in isolated primary mouse hepatocytes and cholangiocytes as well as in MSC and MLC cells (Figures 4C and 5A). Collectively, these results demonstrate the presence of LRRC8A in mouse liver, isolated hepatocytes and cholangiocytes, and MSC and MLC cells.

LRRC8A represents a critical component of the VRAC in mouse cholangiocytes

To characterize and identify the molecular basis of the VRAC in mouse cholangiocytes, whole-cell currents were measured in MLC and MSC cells transfected with LRRC8A siRNA (siLRRC8A) and compared with mock transfected or nontargeting siRNA control transfected cells (siCtrl) (Figure 5 and Figure S1). The efficiency of LRRC8A knockdown was assessed by western blot analysis and demonstrated a decrease in LRRC8A expression by greater than 70% in both MLC and MSC (Figure 5A,B). The cells transfected with siRNA control and bathed in a hypotonic (190 mOsm) solution displayed characteristic volume-activated Cl^- currents. After transfection with LRRC8A siRNA, the volume-activated Cl^- currents were abolished (Figure 5C,D). Note that MSC exhibited similar inhibition of volume-activated Cl^- currents after transfection with LRRC8A siRNA (Figure S1). Together, these studies provide further evidence that LRRC8A contributes to the volume-regulated anion currents in MLCs and MSCs.

Cell swelling precedes LRRC8A activation

In order to confirm the relative sequence of events related to cell volume recovery, simultaneous capacitance (to measure cell volume) and whole-cell patch-clamp studies (to measure Cl^- currents) were performed. The MLC cells demonstrated a significantly greater capacitance than the MSC at baseline in isotonic conditions (Figure 6A). As shown in the representative tracing in Figure 6B, exposure of MLC cells to hypotonicity (190 mOsm) instantaneously increased membrane capacitance (cell volume) followed by a more gradual recovery toward basal levels. The increase in cell capacitance always preceded the activation of Cl^- currents, demonstrating that cell swelling occurs first, followed by activation of membrane Cl^- currents. In this case, the time delay of the current peak from the maximum capacitance value was 1.9 + 0.20 min (n = 14). This is consistent with findings in other cell types, where the initial increase in cell volume is due to rapid and passive influx of water into the cell.[9,13] The initial increase in cell volume is followed by activation of membrane Cl^- channels and a gradual return to basal cell volume. The effect of DCPIB led to a rapid decrease in the amplitude of the current but did not affect the dynamics of changes of the membrane capacitance in response to hypotonicity (Figure 6C). We found

no statistically significant difference in the relative increase of membrane capacitance, in response to hypotonic exposure, between MLCs and MSCs (Figure 6D).

LRRC8A contributes to RVD in mouse cholangiocytes

To measure the contribution of LRRC8A to cell volume recovery, MLC and MSC cells were loaded with the fluorescent dye calcein-AM, exposed to isotonic and hypotonic conditions, and cell volume was measured using the calcein-AM fluorescence self-quenching method.[23,24] To briefly explain the method, a decrease in cell volume leads to an increase in intracellular calcein-AM concentration, which triggers the self-quenching of calcein-AM. The self-quenching of calcein-AM leads to a decrease in cellular fluorescence. The opposite is true for an increase in cell volume, which results in an increase in cellular fluorescence due to the lack of self-quenching. In the presence of an isotonic solution (310 mOsM), MLC and MSC cells had a constant fluorescence intensity over the course of the entire experiment Figure 7A,B). After 3 min, the isotonic solution was replaced with a hypotonic solution (100 mOsm). Bathing of MLC and MSC cells in the hypotonic solution resulted in a rapid increase in cellular fluorescence, which is representative of an increase in cell volume (Figure 7A,B). The rapid increase was followed by a continued decrease in cellular fluorescence toward the basal isotonic fluorescence intensity despite the cells being bathed in a hypotonic solution. The decrease in cellular fluorescence is reflective of a decrease in cell volume through the process of RVD (Figure 7A,B). To evaluate whether the LRRC8/VRAC channel contributes to RVD, the intensity of cellular fluorescence was measured in cells bathed in a hypotonic solution with or without the LRRC8/VRAC antagonist, DCPIB. As shown in Figure 7, DCPIB at a concentration of either 10 or 20 μm significantly inhibited the RVD process in both MLC and MSC cells. The inhibition of RVD in the presence of DCPIB indicates that LRRC8/VRAC channel activity contributes to the RVD process in MLCs and MSCs.

DISCUSSION

These studies identify and functionally characterize LRRC8A as a critical member of the VRAC in mouse cholangiocytes. Evidence for this includes (i) in response to hypotonic exposure, both MSC and MLC increase cell volume, activate membrane Cl^- currents, and undergo RVD; (ii) VRAC currents exhibit time-d ependent inactivation at positive membrane potentials and a reversal at 0 mV, biophysical properties consistent with LRRC8A activation in other cell types; (iii) both MSC and MLC express LRRC8A mRNA, as well as other family members (B, C, D, E); (iv) western blot analysis and immunostaining of whole mouse liver demonstrated LRRC8A protein expression in both hepatocytes and cholangiocytes; (v) both RVD and VRAC currents are inhibited by DCPIB, an LRRC8/VRAC antagonist; (vi) VRAC currents are abolished in cells transfected with LRRC8A siRNA; (vii) LRRC8A mediates Cl^- currents, as removal of Cl^- in the buffer abolishes VRAC currents; and (viii) in all cases, cell swelling preceded Cl^- channel activation as measured by simultaneous whole-cell capacitance and patch-clamp analysis. Together, these results demonstrate that LRRC8A is functionally present in mouse cholangiocytes and contributes to volume-regulated anion secretion and RVD.

Although maintenance of cell volume is an essential function of all cells, especially those of the liver, increasing evidence suggests that changes in cell size *per se* may be a signal influencing cell and organ level functions.[13,25] For example, although the hormone insulin increases hepatocyte cell volume and activates glycogen and protein synthesis, increases in cell volume alone, without insulin, reproduce many of these same metabolic effects.[26,27] Additionally, we have previously shown that a human biliary epithelial cell model activates a volume-regulated Cl^- channel and undergoes RVD when exposed to hypotonic conditions[15] and, in the isolated perfused rat liver model, RVD stimulates bile flow.[12] Together, these findings suggest that liver cell volume changes may represent a signal regulating liver functions. Thus, identification of LRRC8A as a critical component of the VRAC suggests that this protein may represent a means of coupling changes in cell volume to cellular metabolism and bile flow. Additionally, as Cl^- channels in the cholangiocyte apical membrane provide the driving force for biliary secretion, Cl^-/HCO_3^- exchange and bile alkalinization, LRCC8A may play an important role in the protective biliary bicarbonate umbrella,[28,29] though clearly more work is needed.

If these studies performed in murine cholangiocyte cell models are applicable to human cells, then several questions as well as uncertainties are raised. First, the subunit composition of functional channels in cholangiocytes is unknown. Previous studies suggest that functional channels are formed by LRRC8 family members arranged in multimers.[16,21,30] Although family member “A” is critical for volume-activated Cl^- channel function, it requires at least one other family member to form a functional channel.[16] Interestingly, the specific combination of LRRC8 family members may confer different biophysical properties to the channel.[30] For example, in other cell types “E” confers a unique pattern to deactivation kinetics, whereas “D” seems to be the important member for volume regulation.[16,21] In our studies, we have identified the presence of all five family members in cholangiocytes by PCR, though “E” was of much lower abundance. Further, we confirmed that “A” was the critical member for volume-dependent activation as knockdown of LRRC8A with siRNA abolished volume-activated Cl^- currents. Further studies are needed to define the functional composition of LRRC8 channels and stoichiometry in cholangiocytes during both physiological and pathological conditions.

Second, the mechanism by which hypotonicity activates LRRC8A is unknown. Is it through mechanosensation and membrane stretch or through changes in intracellular ionic strength? Both hypotheses may be relevant as determined by other studies.[30,31] It may be that membrane stretch or distention transduces through the leucine-rich-repeat domain (LRRD) at the C-terminal end of the protein to assert mechanical effects on the LRRDs on adjacent LRRC8 subunits, thus opening the pore and activating the channel.[31] In contrast, a decrease in intracellular ionic strength activates VRACs in endothelial cells[32,33] and in Chinese hamster ovary cells.[34] In fact, both processes may be necessary and a decrease in intracellular ionic strength may influence the set-point for activation of the channel on mechanical distention.[34] Our studies, which simultaneously measure both capacitance (as a reflection of cell size) and ion channel activity, demonstrate that increases in cell size always precede channel activation and thus could be consistent with both hypotheses. It should be noted, however, that cholangiocytes express other mechanosensitive channels, including transient receptor potential vanilloid member 4,[35] which translate changes in fluid-flow at

the apical membrane to increases in [Ca^{2+}] and Cl^- channel activity.[35,36] Thus, it is not only feasible, but likely, that membrane distention is one of the critical stimuli necessary for cholangiocyte LRRC8A activation, though further work is needed.

Third, although a recent study using FRET-based analysis of channel activity demonstrated that protein kinase D is critically involved in LRRC8A activity,[37] the kinase signaling pathways involved in LRRC8A regulation in cholangiocytes is unknown. Previously, we have shown important roles of protein kinase C (PKC) in both VRAC and TMEM16A Cl^- channel activation.[38,39] In fact, PKCα is rapidly translocated from the cytosol to the plasma membrane on stimulation by fluid-flow or hypotonicity in both hepatocyte and cholangiocyte cell models, and inhibition of PKC abolishes mechanical- and volume-regulated channel activation.[38,39] Furthermore, we have demonstrated an important role for phosphoinositide-3 kinase (PI3K) in VRAC activity because the downstream lipid products of PI3K activate Cl^- channels in response to hypotonicity in a human biliary model.[15] The role of kinase signaling in LRRC8A regulation requires additional study.

Lastly, given the link between cell volume changes and cellular metabolism, targeting LRRC8A may represent a therapeutic modality in the treatment of metabolic disease. For example, it has previously been shown that LRRC8A expression in adipocytes increases during obesity, and knockdown of LRRC8A in high-fat diet–fed mice results in increased weight gain, increased adiposity, and worse insulin resistance.[40,41] These findings suggest that LRRC8A plays a protective role during fat accumulation and obesity; however, its role in the development or progression of NAFLD is unknown and will require further study. Overall, although further studies are needed, the molecular identification of LRRC8A in cholangiocytes is an important first step in unraveling hepatobiliary function and coupling cellular membrane transport to organ level function in liver health and disease.

Supplementary Material

Refer to Web version on PubMed Central for supplementary material.

ACKNOWLEDGMENTS

The authors wish to thank Dr. Gianfranco Alpini and Dr. Shannon Glaser for supplying the MSC and MLC cells and William C. Bowen and Dr. George K. Michalopoulos for supplying the primary hepatocytes.

Funding information

Supported by the Hillman Cancer Center and Tissue and Research Pathology, Pitt Biospecimen Core of the University of Pittsburgh, the Carol Ann Craumer Endowed Chair in Pediatric Research, the Department of Pediatrics, the Pittsburgh Liver Research Center, the Cystic Fibrosis Foundation (FERANC21P0), and the National Institute of Diabetes, Digestive and Kidney Diseases of the National Institutes of Health under award number P30DK120531 and award number R01DK078587 (to Andrew P. Feranchak). The Tissue and Research Pathology Pitt Biospecimen Core is supported in part by award P30CA047904 from the National Institutes of Health. The content is solely the responsibility of the authors and does not necessarily represent the official views of the National Institutes of Health.

Abbreviations:

CaCl2	calcium chloride

cDNA	complementary DNA
CFTR	cystic fibrosis transmembrane conductance regulator
DCPIB	4-[(2-butyl-6,7-dichloro-2-cyclopentyl-2,3-dihydro-1-oxo-1H-inden-5-y l) oxy] butanoic acid
LRRC8A	leucine-rich repeat-containing protein 8, subfamily A
MgCl2	magnesium chloride
MLC	mouse large cholangiocytes
MSC	mouse small cholangiocytes
NaCl	sodium chloride
PKC	protein kinase C
RT-PCR	reverse transcription polymerase chain reaction
RVD	regulatory volume decrease
siLRRC8A	LRRC8A siRNA
siRNA	small interfering RNA
TMEM16A	transmembrane member 16A protein
VRAC	volume-regulated anion channel

REFERENCES

1. Kumar U, Jordan TW. Isolation and culture of biliary epithelial cells from the biliary tract fraction of normal rats. Liver. 1986;6(6):369–78. [PubMed: 3574003]
2. Nathanson MH, Boyer JL. Mechanisms and regulation of bile secretion. Hepatology. 1991;14(3):551–66. [PubMed: 1874500]
3. Fitz JG. Regulation of cholangiocyte secretion. Semin Liver Dis. 2002;22(3):241–9. [PubMed: 12360418]
4. Dutta AK, Woo K, Doctor RB, Fitz JG, Feranchak AP. Extracellular nucleotides stimulate Cl- currents in biliary epithelia through receptor-mediated IP3 and Ca2+ release. Am J Physiol Gastrointest Liver Physiol. 2008;295(5):G1004–G1015. [PubMed: 18787062]
5. Fitz JG, Basavappa S, McGill J, Melhus O, Cohn JA. Regulation of membrane chloride currents in rat bile duct epithelial cells. J Clin Invest. 1993;91(1):319–28. [PubMed: 7678606]
6. Basavappa S, Middleton J, Mangel AW, McGill JM, Cohn JA, Fitz JG. Cl− and K+ transport in human biliary cell lines. Gastroenterology. 1993;104(6):1796–805. [PubMed: 7684717]
7. Cohn JA, Strong TA, Picciotto MA, Nairn AC, Collins FS, Francis S, et al. Localization of CFTR in human bile duct epithelial cells. Gastroenterology. 1993;105(6):1857–64. [PubMed: 7504645]
8. Dutta AK, Khimji AK, Kresge C, Bugde A, Dougherty M, Esser V, et al. Identification and functional characterization of TMEM16A, a Ca2+-activated Cl- channel activated by extracellular nucleotides, in biliary epithelium. J Biol Chem. 2011;286(1):766–76. [PubMed: 21041307]
9. Qiu Z, Dubin A, Mathur J, Tu B, Reddy K, Miraglia L, et al. SWELL1, a plasma membrane protein, is an essential component of volume-regulated anion channel. Cell. 2014;157(2):447–58. [PubMed: 24725410]

10. Pedersen SF, Okada Y, Nilius B. Biophysics and physiology of the volume-regulated anion channel (VRAC)/volume-sensitive outwardly rectifying anion channel (VSOR). Pflügers Arch. 2016;468(3):371–83. [PubMed: 26739710]
11. Syeda R, Qiu Z, Dubin A, Murthy S, Florendo M, Mason D, et al. LRRC8 proteins form volume-regulated anion channels that sense ionic strength. Cell. 2016;164(3):499–511. [PubMed: 26824658]
12. Bruck R, Haddad P, Graf J, Boyer JL. Regulatory volume decrease stimulates bile flow, bile acid excretion, and exocytosis in isolated perfused rat liver. Am J Physiol. 1992;262(5):G806–12. [PubMed: 1590390]
13. Dunkelberg JC, Feranchak AP, Fitz JG. Liver cell volume regulation: size matters. Hepatology. 2001;33(6):1349–52. [PubMed: 11391521]
14. Hoffmann EK, Holm NB, Lambert IH. Functions of volume-sensitive and calcium-activated chloride channels. IUBMB Life. 2014;66(4):257–67. [PubMed: 24771413]
15. Feranchak AP, Roman RM, Doctor RB, Salter KD, Toker A, Fitz JG. The lipid products of phosphoinositide 3-kinase contribute to regulation of cholangiocyte ATP and chloride transport. J Biol Chem. 1999;274(43):30979–86. [PubMed: 10521494]
16. Voss FK, Ullrich F, Münch J, Lazarow K, Lutter D, Mah N, et al. Identification of LRRC8 heteromers as an essential component of the volume-regulated anion channel VRAC. Science. 2014;344(6184):634–8. [PubMed: 24790029]
17. Glaser S, Wang M, Ueno Y, Venter J, Wang K, Chen H, et al. Differential transcriptional characteristics of small and large biliary epithelial cells derived from small and large bile ducts. Am J Physiol Gastrointest Liver Physiol. 2010;299(3):G769–G777. [PubMed: 20576918]
18. Ueno Y, Alpini G, Yahagi K, Kanno N, Moritoki Y, Fukushima K, et al. Evaluation of differential gene expression by microarray analysis in small and large cholangiocytes isolated from normal mice. Liver Int. 2003;23(6):449–59. [PubMed: 14986819]
19. Decher N, Lang HJ, Nilius B, Bruggemann A, Busch AE, Steinmeyer K. DCPIB is a novel selective blocker of I(Cl, swell) and prevents swelling-induced shortening of guinea-pig atrial action potential duration. Br J Pharmacol. 2001;134(7):1467–79. [PubMed: 11724753]
20. Yamada T, Figueroa EE, Denton JS, Strange K. LRRC8A homohexameric channels poorly recapitulate VRAC regulation and pharmacology. Am J Physiol Cell Physiol. 2021;320(3):C293–C303. [PubMed: 33356947]
21. Jentsch TJ, Lutter D, Planells-Cases R, Ullrich F, Voss FK. VRAC: molecular identification as LRRC8 heteromers with differential functions. Pflügers Arch. 2016;468(3):385–93. [PubMed: 26635246]
22. Osei-Owusu J, Yang J, Vitery MDC, Qiu Z. Molecular biology and physiology of volume-regulated anion channel (VRAC). Curr Top Membr. 2018;81:177–203. [PubMed: 30243432]
23. Friard J, Tauc M, Cougnon M, Compan V, Duranton C, Rubera I. Comparative effects of chloride channel inhibitors on LRRC8/VRAC-mediated chloride conductance. Front Pharmacol. 2017;8:328. [PubMed: 28620305]
24. Capo-Aponte JE, Iserovich P, Reinach PS. Characterization of regulatory volume behavior by fluorescence quenching in human corneal epithelial cells. J Membr Biol. 2005;207(1):11–22. [PubMed: 16463139]
25. Häussinger D, Schliess F. Osmotic induction of signaling cascades: role in regulation of cell function. Biochem Biophys Res Commun. 1999;255(3):551–5. [PubMed: 10049748]
26. Schliess F, Häussinger D. Cell hydration and insulin signalling. Cell Physiol Biochem. 2000;10(5–6):403–8. [PubMed: 11125222]
27. Häussinger D, Schliess F, Dombrowski F, Vom Dahl S. Involvement of p38MAPK in the regulation of proteolysis by liver cell hydration. Gastroenterology. 1999;116(4):921–35. [PubMed: 10092315]
28. Hohenester S, Wenniger LM, Paulusma CC, van Vliet SJ, Jefferson DM, Elferink RP, et al. A biliary HCO3- umbrella constitutes a protective mechanism against bile acid-induced injury in human cholangiocytes. Hepatology. 2012;55(1):173–83. [PubMed: 21932391]

29. Beuers U, Hohenester S, de Buy Wenniger LJM, Kremer AE, Jansen PLM, Elferink RPJO. The biliary HCO(3)(−) umbrella: a unifying hypothesis on pathogenetic and therapeutic aspects of fibrosing cholangiopathies. Hepatology. 2010;52(4):1489–96. [PubMed: 20721884]
30. Konig B, Stauber T. Biophysics and structure-function relationships of LRRC8-formed volume-regulated anion channels. Biophys J. 2019;116(7):1185–93. [PubMed: 30871717]
31. Strange K, Yamada T, Denton JS. A 30-year journey from volume-regulated anion currents to molecular structure of the LRRC8 channel. J Gen Physiol. 2019;151(2):100–17. [PubMed: 30651298]
32. Voets T, Droogmans G, Raskin G, Eggermont J, Nilius B Reduced intracellular ionic strength as the initial trigger for activation of endothelial volume-regulated anion channels. Proc Natl Acad Sci U S A. 1999;96(9):5298–303. [PubMed: 10220460]
33. Sabirov RZ, Merzlyak PG, Islam MR, Okada T, Okada Y. The properties, functions, and pathophysiology of maxi-anion channels. Pflugers Arch. 2016;468(3):405–20. [PubMed: 26733413]
34. Cannon CL, Basavappa S, Strange K. Intracellular ionic strength regulates the volume sensitivity of a swelling-activated anion channel. Am J Physiol. 1998;275(2):C416–C422. [PubMed: 9688595]
35. Li Q, Kresge C, Boggs K, Scott J, Feranchak A. Mechanosensor transient receptor potential vanilloid member 4 (TRPV4) regulates mouse cholangiocyte secretion and bile formation. Am J Physiol Gastrointest Liver Physiol. 2020;318(2):G277–G287. [PubMed: 31760763]
36. Dutta AK, Woo K, Khimji AK, Kresge C, Feranchak AP. Mechanosensitive Cl- secretion in biliary epithelium mediated through TMEM16A. Am J Physiol Gastrointest Liver Physiol. 2013;304(1):G87–G98. [PubMed: 23104560]
37. König B, Hao Y, Schwartz S, Plested AJ, Stauber T. A FRET sensor of C-terminal movement reveals VRAC activation by plasma membrane DAG signaling rather than ionic strength. eLife. 2019;8:e45421.
38. Roman RM, Bodily KO, Wang Y, Raymond JR, Fitz JG. Activation of protein kinase Calpha couples cell volume to membrane Cl- permeability in HTC hepatoma and Mz-ChA-1 cholangiocarcinoma cells. Hepatology. 1998;28(4):1073–80. [PubMed: 9755245]
39. Dutta AK, Khimji AK, Liu S, Karamysheva Z, Fujita A, Kresge C, et al. PKCα regulates TMEM16A-mediated Cl(−) secretion in human biliary cells. Am J Physiol Gastrointest Liver Physiol. 2016;310(1):G34–G42. [PubMed: 26542395]
40. Zhang Y, Xie L, Gunasekar SK, Tong D, Mishra A, Gibson WJ, et al. SWELL1 is a regulator of adipocyte size, insulin signalling and glucose homeostasis. Nat Cell Biol. 2017;19(5):504–17. [PubMed: 28436964]
41. Xie L, Zhang Y, Gunasekar SK, Mishra A, Cao L, Sah R. Induction of adipose and hepatic SWELL1 expression is required for maintaining systemic insulin-sensitivity in obesity. Channels (Austin). 2017;11(6):673–7. [PubMed: 28873008]

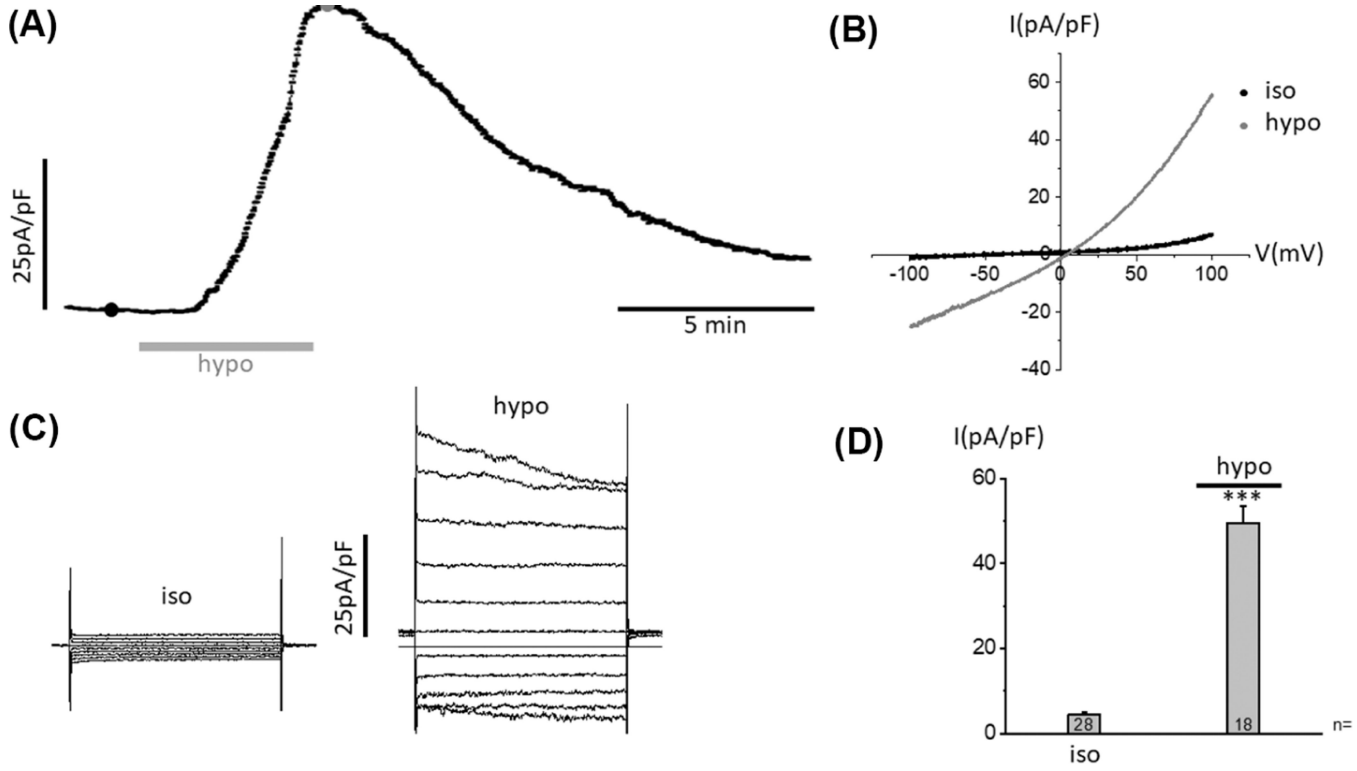

FIGURE 1.

Increased VRAC in cholangiocytes, exposed in hypotonicity. (A) In this representative whole-cell recording from MLCs, current was measured at +100 mV every 2 s. (B) Current/Voltage curves correspond with black and gray circles on current trace. (C) Current traces obtained from 400 ms step starting from −100 to +100 mV in 20 mV increments. (D) The bar graph summarizes current density data measured at +100 mV (mean ± SE). ***$p <$ 0.001

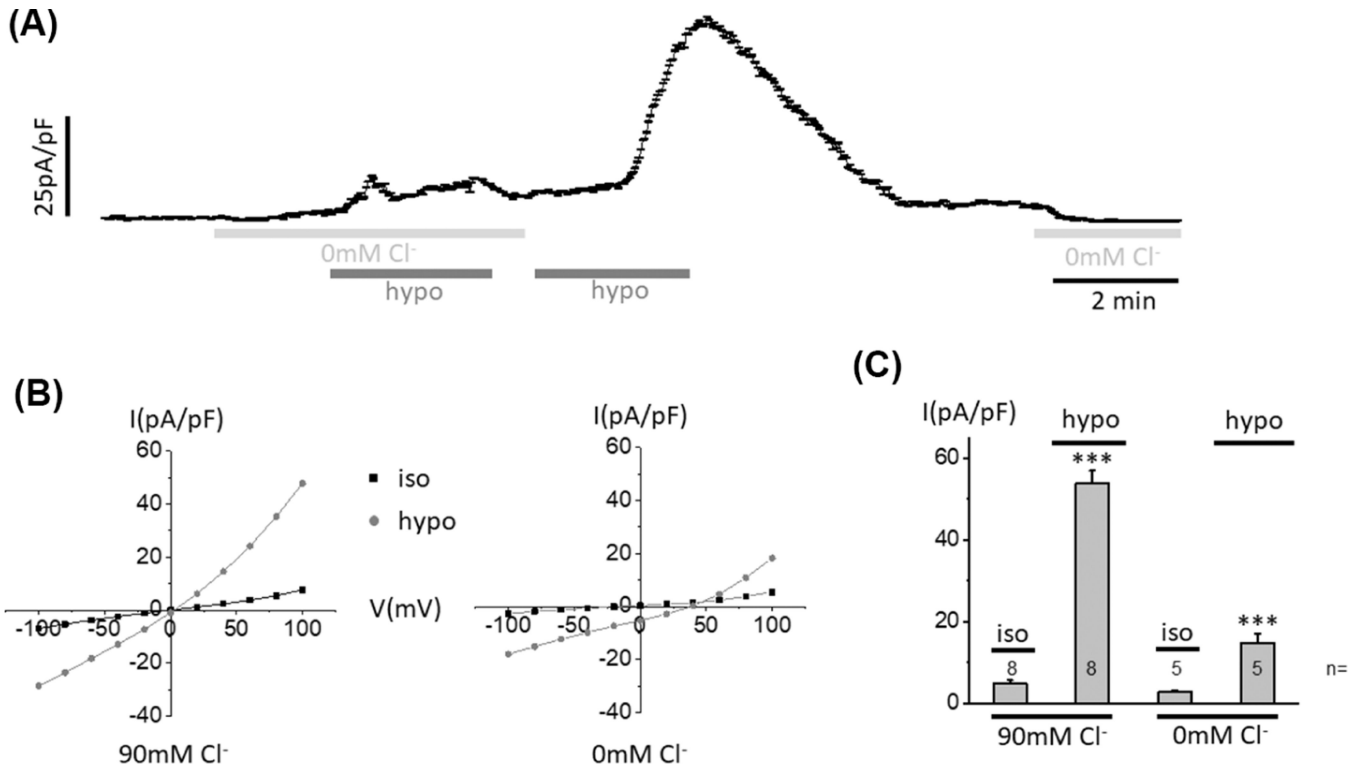

FIGURE 2.

Dependence of VRAC on the presence of chloride ions in the bath solution. (A) Comparison of currents caused by sequential cell treatment with hypotonic solution without chloride ions and a solution with normal chloride concentration. (B) Current–voltage relationship between normal and chloride-free conditions using step protocol. (C) Summarized current densities at +100 mV. ***$p < 0.001$

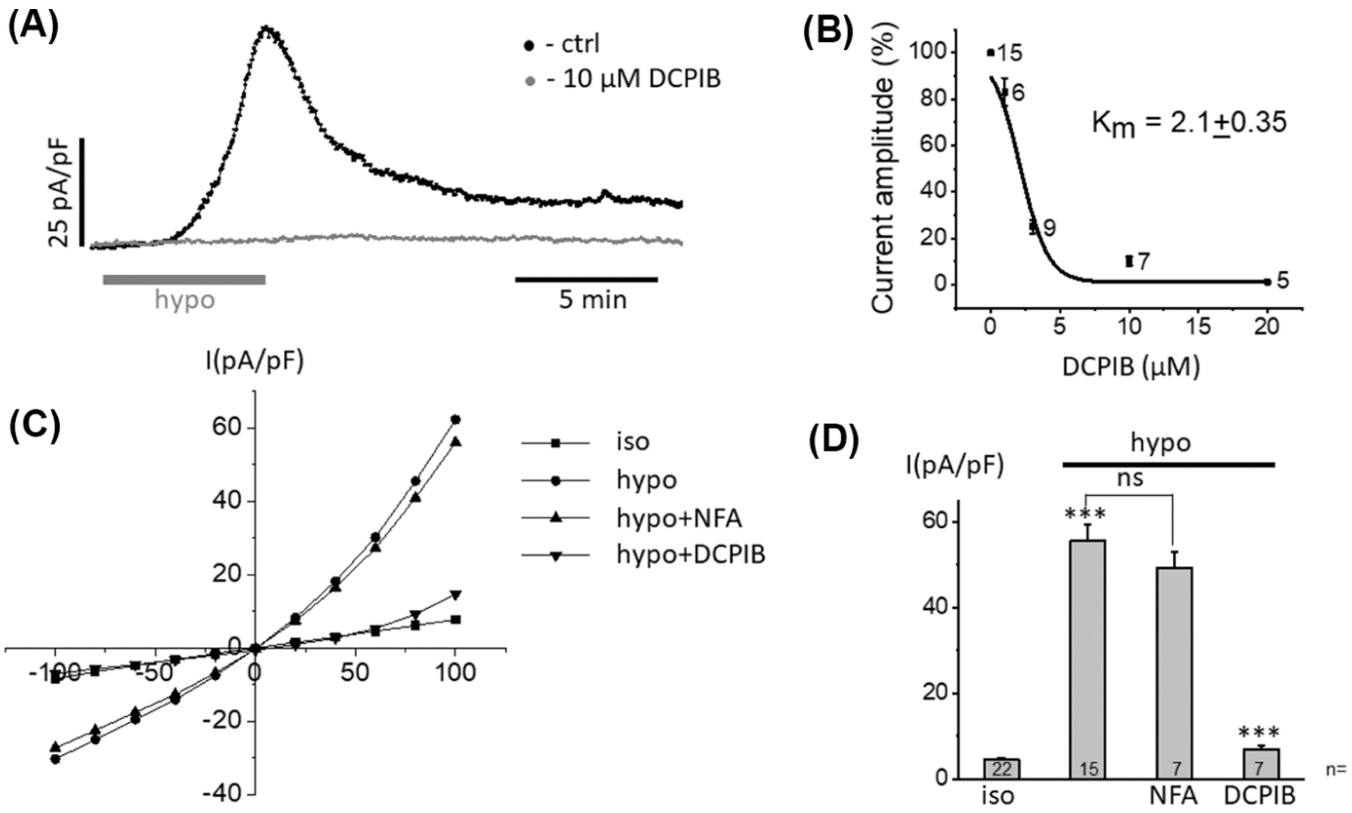

FIGURE 3.

Inhibition of LRRC8/VRAC channel activity by DCPIB. (A,B) Pretreatment of cell with solution containing 10 μm DCPIB (specific blocker of LRRC8A channel) completely abolished cell response to hypotonicity with K_m = 2.1 + 0.35 μm. (C) NFA at concentration of 100 μm did not have a significant effect on VRAC current (P_{val} = 0.2824). (D) The summary data of inhibitor effects are shown. ***$p < 0.001$

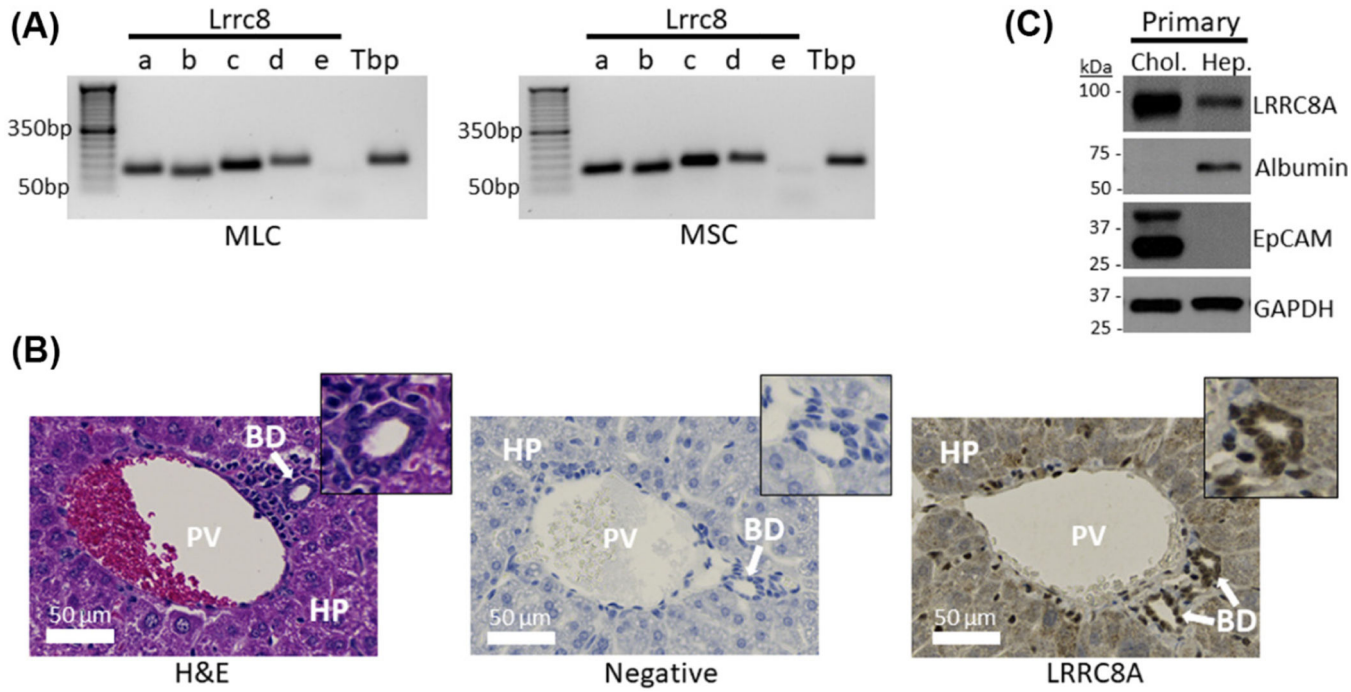

FIGURE 4.

LRRC8A expression in cholangiocytes. (A) RT-PCR of Lrrc8 paralogs (Lrrc8a–e) in MLC and MSC cells. TATA-binding protein (Tbp) is a control. (B) Hematoxylin and eosin (H&E) staining of the liver. Immunohistochemistry staining for LRRC8A protein in whole mouse liver. Arrows and insets highlight the cholangiocytes that line the bile duct. Scale bar represents 50 µm (40× magnification). (C) Western blot on primary murine cholangiocytes and hepatocytes showing LRRC8A, cholangiocyte-specific EpCAM, and hepatocyte-specific albumin protein expression levels. GAPDH was used as a loading control. BD, bile duct; HP, hepatocytes; PV, portal vein

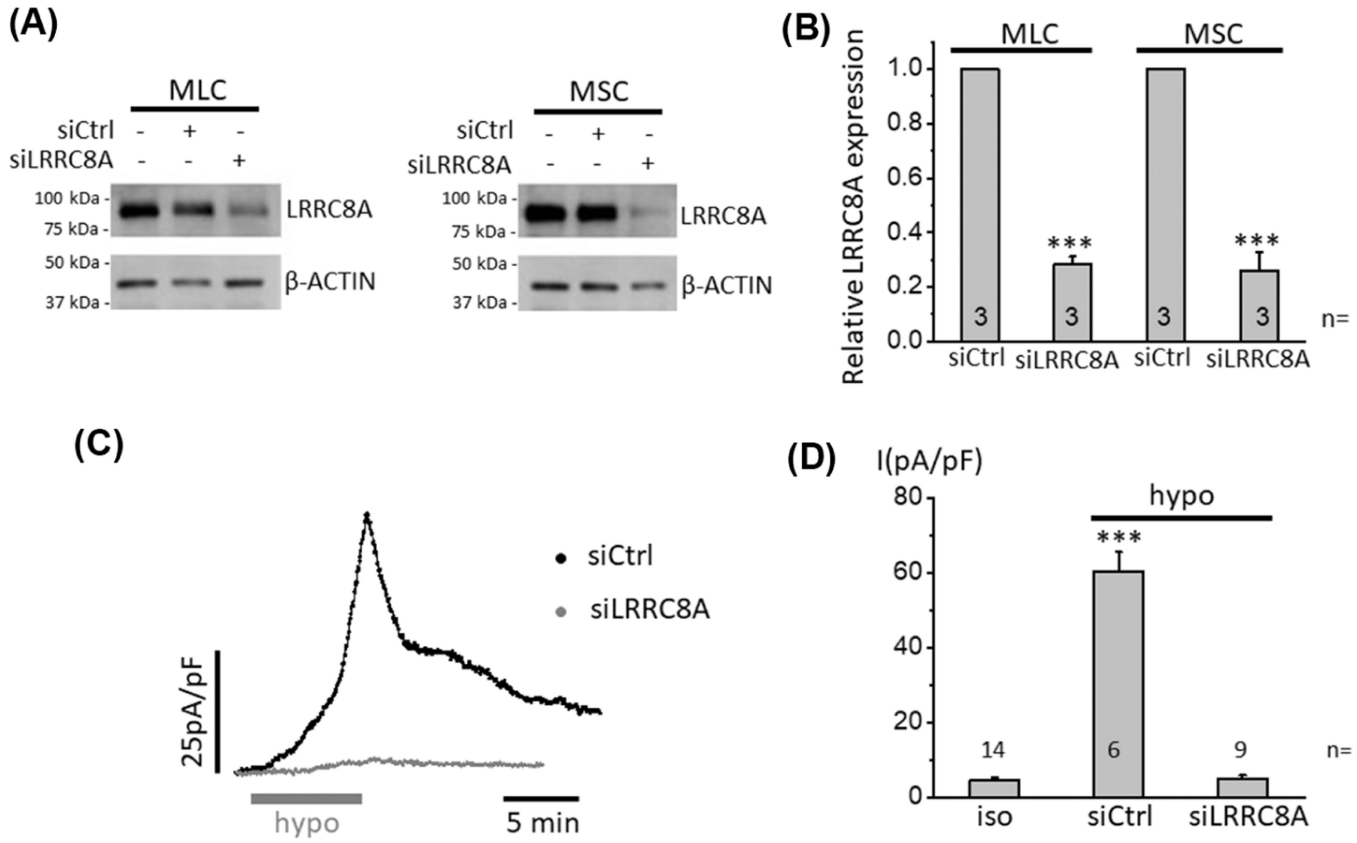

FIGURE 5.

Knockdown of LRRC8A decreases LRRC8A protein expression and LRRC8/VRAC channel activity in cholangiocytes. (A) A representative western blot showing a decrease in LRRC8A protein expression 48 h after siLRRC8A transfection in both MLC and MSC cells compared with mock or control siRNA (siCtrl) transfections. β-Actin serves as the loading control. (B) Cumulative data showing LRRC8A protein expression after 48 h after siLRRC8A transfection relative to control siRNA transfections in both MLC and MSC cells. The error bars represent ± SE; $n = 3$; and ***$p < 0.001$. (C) Whole-cell currents at +100 mV induced by hypotonic solution in MLCs transfected with LRRC8A siRNA versus siRNA control. (D) Summarize current densities at +100 mV. ***$p < 0.001$

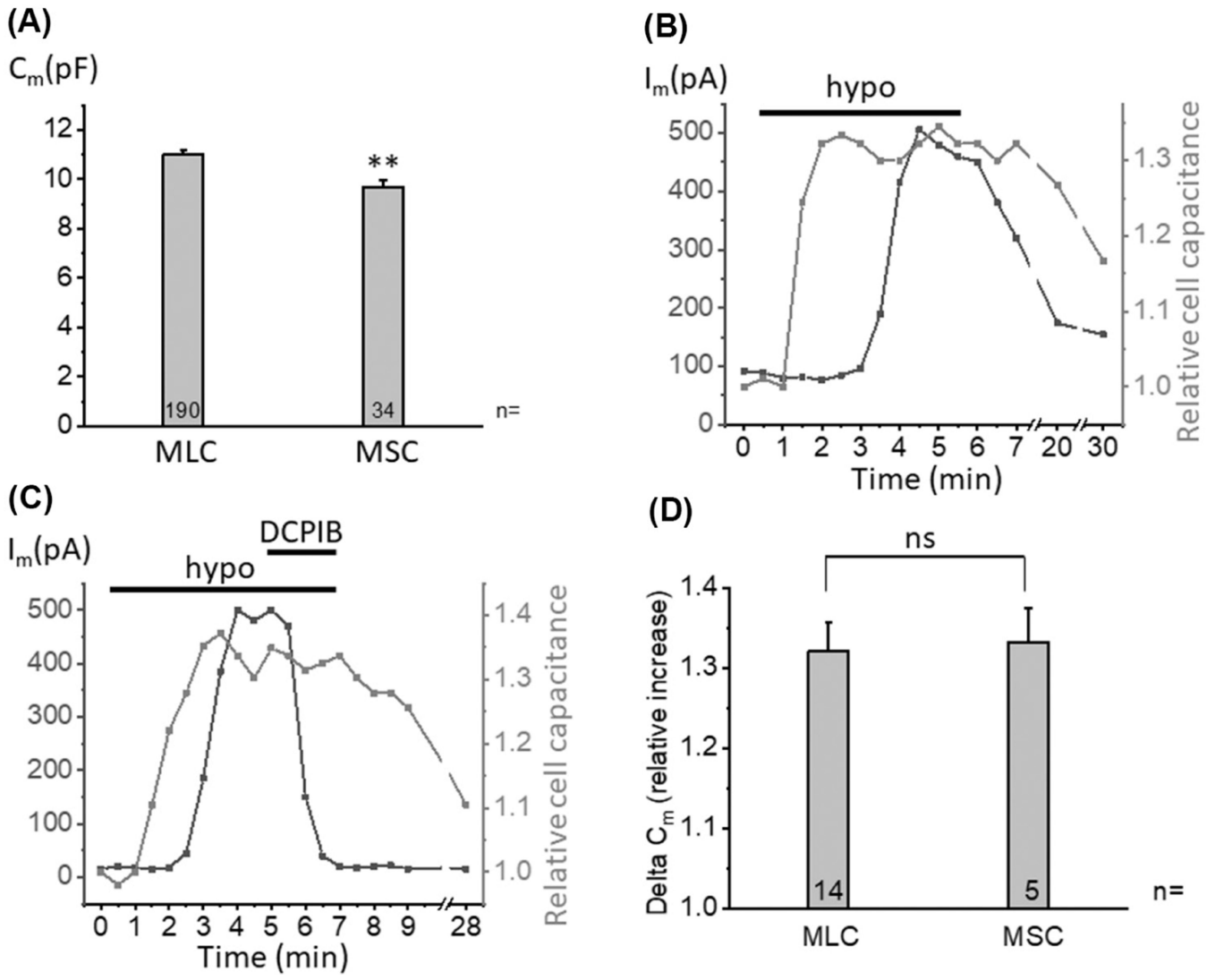

FIGURE 6.

Relationship between LRRC8/VRAC channel activation, RVD, and cell capacitance in cholangiocytes. (A) Comparative capacity of MLCs (11.0 + 0.19 pF) and MSCs (9.7 + 0.24 pF) in normal isotonic solution. The mean of group one minus group two in (D) equals 1.3000 pF, $^{**}p < 0.01$. (B) Relative cell capacitance is measured simultaneously with whole-cell current, allowing a direct correlation between VRAC activation and cell capacitance, which is the signal that activates the channel. (C) Effect of 10 μm DCPIB on VRAC and cell capacitance. (D) Summarized delta of relative increase of cell capacitance in iso- and hypotonic solutions for MLCs and MSCs

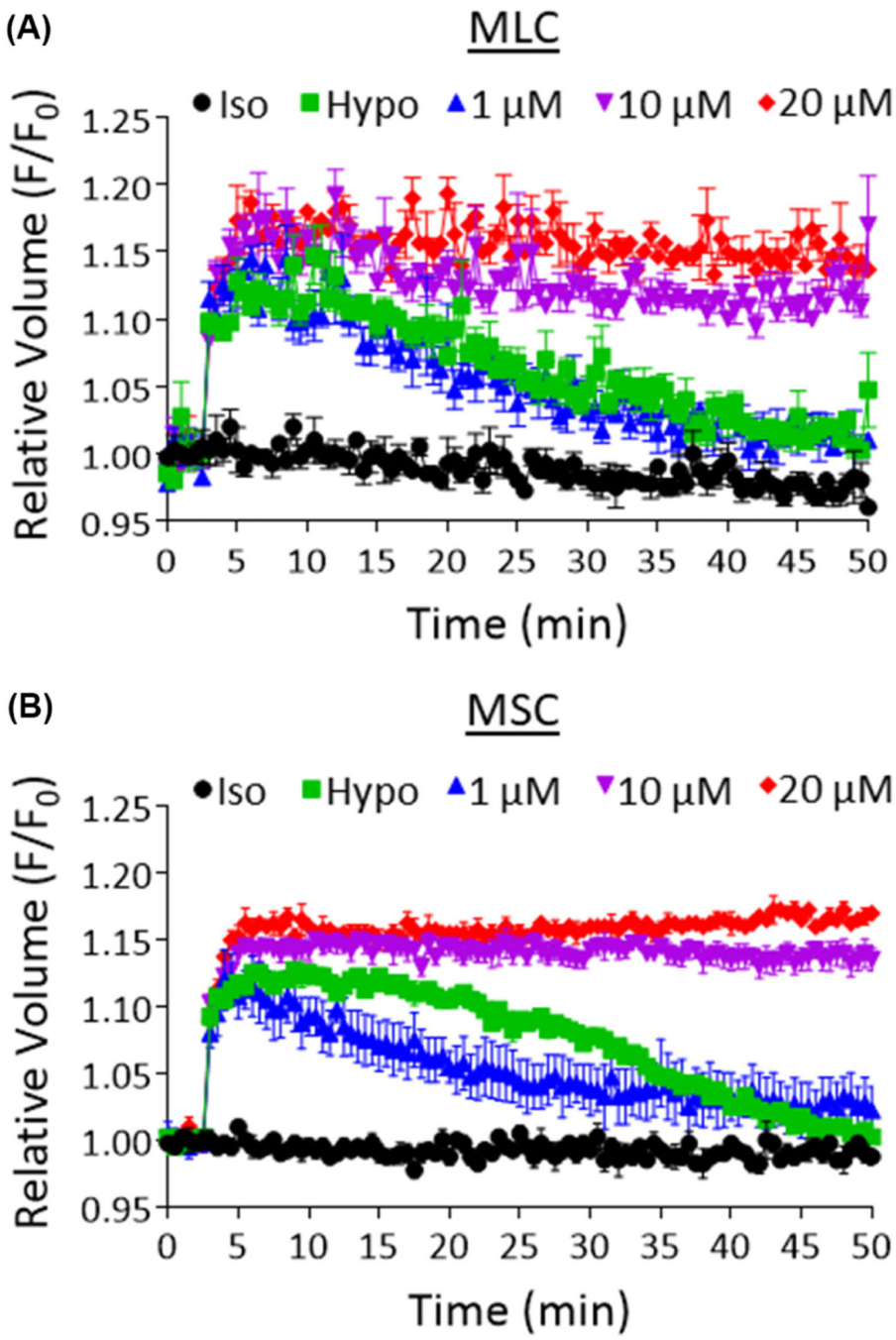

FIGURE 7.

Relationship between LRRC8/VRAC channel activation, RVD, and cell capacitance in cholangiocytes. Quantitative measurement of RVD in (A) MLC and (B) MSC cells. Black data points represent fluorescence intensity in cells bathed in 310 mOsm isotonic solution for the entire experiment. Green data points represent fluorescence intensity in cells bathed in 310 mOsm isotonic solution for 3 min followed by a 100 mOsm hypotonic bath solution for the next 47 min. The blue, purple, and red data points represent fluorescence intensity of cells with the addition of 1, 10, or 20 μm DCPIB, respectively, to the 100 mOsm hypotonic

bath solution. Data are relative to the baseline isotonic reading (black). The error bars represent ± SE; n = 4 wells (40,000 cells per well)